

CALIFORNIA INSTITUTE OF TECHNOLOGY

PASADENA, CALIFORNIA 91125

December 01, 2007 (revised December 17)

To: MWA-LFD Collaboration

From: Judd D. Bowman

Subject: Analysis of Drift Scans From 32T-X1 and Characterization of System Temperature

1. Introduction

Three long drift scans with separate antenna tiles were acquired during the X1 antenna deployment campaign at Boolardy Station between November 13 and November 16, 2007. The goal of the observations was to provide data necessary to characterize the gain and receiver temperature of the antenna tiles. The three configurations used are summarized below (adapted from Jamie Stevens' log descriptions):

1. *firsttile*. The RF switch was connected and enabled in software so that both polarizations could be obtained semi-concurrently from tile 16. For this test, polarization 1 was north-south aligned and phased to point at the zenith (actually, the delay lines in the beamformer were completely passed for polarization 1), while polarization 2 was aligned east-west and phased (using the delay lines in the beamformer this time) to point at $az=180$, $za=10$ degrees. (Note: the log description in the data directory contradicts the polarization states for this data file, but due to a number of supporting pieces of evidence, we are confident the description here is correct.) The observations span approximately 6 hours, including the time of Galactic center transit. These measurements required decreasing the time stamp by 0.1 hours in order to align with the models. This was not a surprise as the field crew expected a 1 to 2 hour offset between the time stamps and UTC. However, both of the other drift scans (see below) required increasing the time stamp of the data by 1.75 hours. The discrepancy is unexplained. In all cases, determining the shift of the time stamps was done by eye.

Files: `firsttile_bothpols_galdrift_2007_317_03.acq`

2. *secondtile*. The beamformer was altered to bypass the delay lines for both polarizations, and moved to tile 15, which had cut (C) dipoles (see EDGES memoranda #30–33 by Alan Rogers). The polarization alignment was unchanged from the *firsttile* measurements (polarization 1 = north-south, polarization 2 = east-west). The observations span approximately 24 hours. This is by far the most useful set of observations because it includes both times of peak emission when the Galactic center transits and times when the emission is near the minimum. Thus, it provides the best constraints on the gain and system temperature. The time stamp on these data needed to be increased by approximate 1.75 hours to align to the models.

Files: `secondtile_galdrift_2007_318_02.acq`
 `secondtile_longdrift_2007_318_08.acq`
 `secondtile_longdrift_2007_319_00.acq`

3. *rfchokeson*. The beamformer was moved back to the first tile (tile 16), and RF chokes were attached to each cable coming from the dipole (as close as possible to the dipole). Again polarization 1 = north-south and polarization 2 = east-west. The observations span approximately 18 hours, without complete profile during Galactic center transit. The time stamp on these data needed to be increased by approximate 1.75 hours to align to the models.

Files: tile16_rfchokeson_longdrift_2007_319_05.acq

All observations were acquired with an Acqiris 8-bit analog-to-digital conversion (ADC) unit (see the EDGES memoranda for details on this instrument). One of the prototype beamformers from the Early Deployment campaigns was used for these measurements. The “polarization” label (1 or 2) used in the descriptions above refers to the input number on the ADC. The north-south or east-west alignment of the antenna tile and any other relevant information for a particular polarization input are given above specifically for each data file.

The sampling code implemented for the Acqiris produces 1-second integrations with 16384 spectral channels between 0 and 500 MHz. The instrument sets a flag for any integration where the ADC overflowed and a separate flag for any where the accumulator overflowed. For the *firsttile* measurements, approximately 10% of the individual 1-second spectra were flagged as including an ADC overflow. Similarly, the *secondtile* and *rfchokes* had approximately 3% and 16% of the individual spectra flagged, respectively. I do not believe any spectra had an accumulator overflow. All individual spectra with an overflow flag were discarded before processing the drift scans. The remaining individual spectra were then integrated into 45-second long observations to reduce the data volume. An additional cut was made at this point by discarding any 45-second spectra with total integrated power over the entire band that deviated by more than approximately 5-sigma from the typical level. Finally, a median filter was applied to each spectrum to retain only the baseband spectrum and reduce the significance of RFI in individual spectral channels. Figure 1 illustrates a typical 45-second spectrum in both its initial state and after filtering. This processing did not remove the effects of the strong RFI at ~250 MHz.

The next six Figures (2 – 7) show the drift scans derived from the observations (black) and the best model fits (blue) based on ideal antenna patterns and the all-sky radio map of Haslam et al. (1982). The plots show drift scans (from top to bottom) between ~75 and 300 MHz in ~3 MHz steps. The large peak in each scan between about 06:00 and 07:00 UTC is due to the Galactic center transiting. The accompanying valley between 09:00 and 18:00 UTC is when very little of the Galactic plane is visible in the beam. The small peak at approximately ~19:00 UTC is attributed to the portion of the Galactic plane roughly opposite the Galactic center transiting. The very small peak at ~4:00 UTC is due to the sun. In general, the model used, based on conical dipoles with no mutual coupling, was a reasonable fit except for three aspects: 1) Although the sun was included as a component of the model, the peak produced by the model seemed to occur a few minutes later than in the measured drift scans. I do not believe this influence the derived gain and system temperature values, though, because the sun contributed neither to the absolute peak (when the Galactic center transited) nor minimum (when the high

Galactic latitude cold sky transited) during a drift scan. 2) The amplitude of the minor peak when the Galactic plane opposite the Galactic center transited was not as strong in the models as in the observations (particularly at lower frequencies), hence the poor match between the blue and black curves at ~18:00 UTC. And finally, 3) there is significant structure in the drift scans during the time of the Galactic center transit that is unexplained. Careful inspection of the *secondtile* measurements also shows a small discontinuous step in the amplitude at about 16:00 UTC.

For the most part, solar flux variation, cloud shadows, and other environmental factors have been ruled out as the sources of the discrepancies. One or a few bright sources in the Galactic center experiencing scintillation would not produce variations on the ~30 minute times scales observed. Also, we don't think the gain of the Acqiris (or any amplifier in the system) would vary with sufficient amplitude to produce the ~5% structure seen during Galactic center transit.

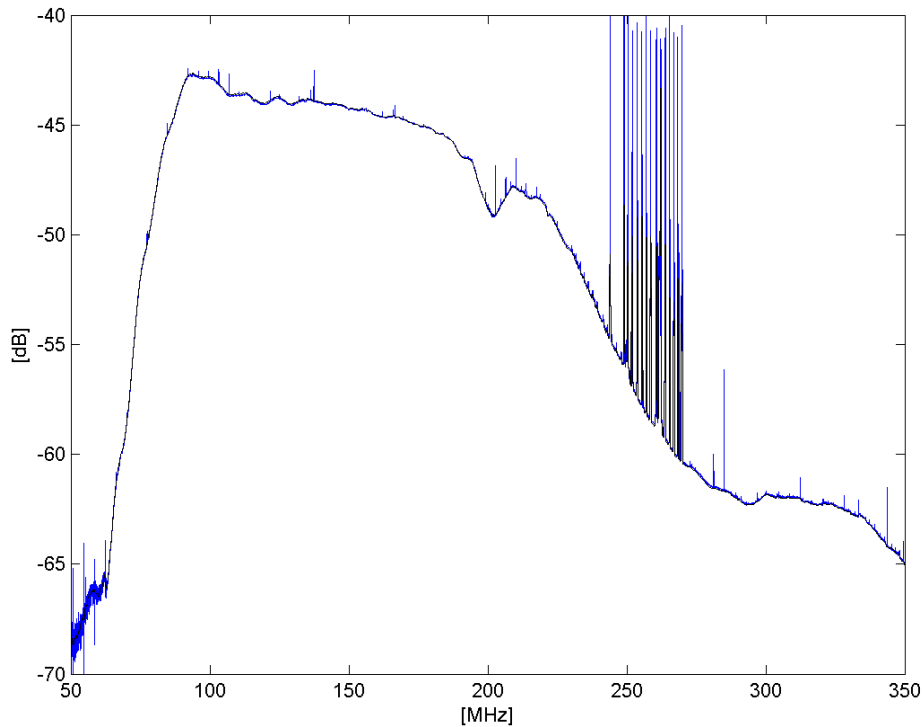
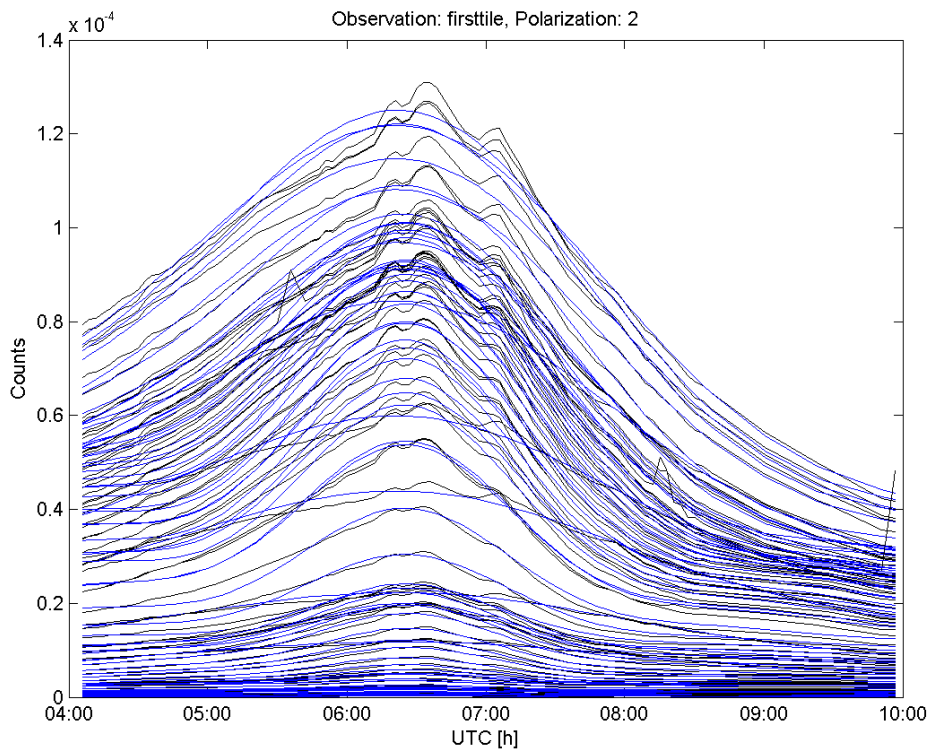
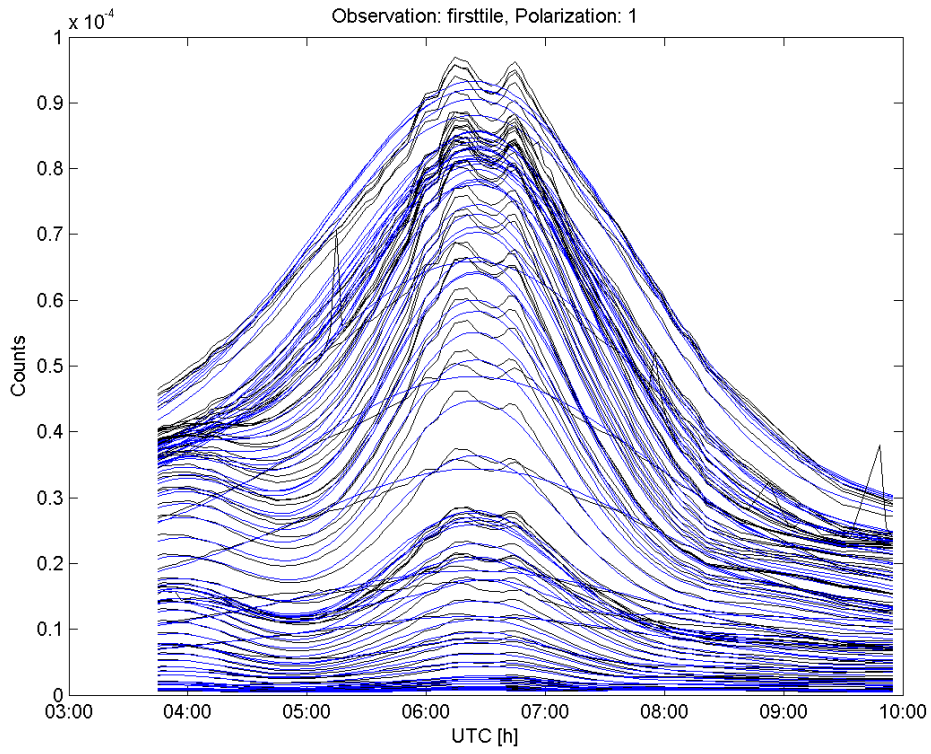
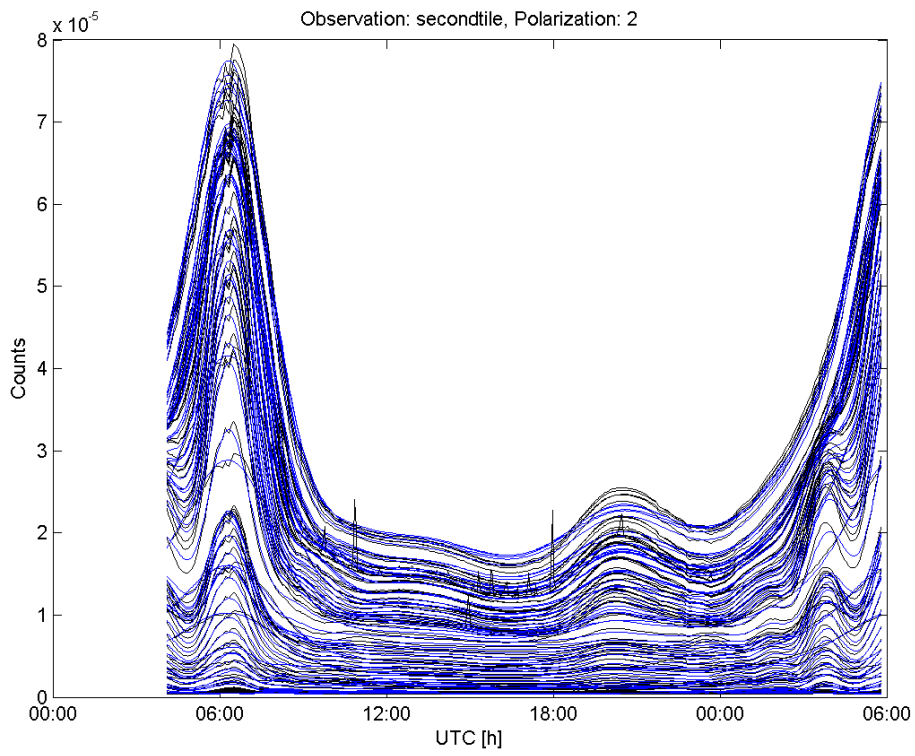
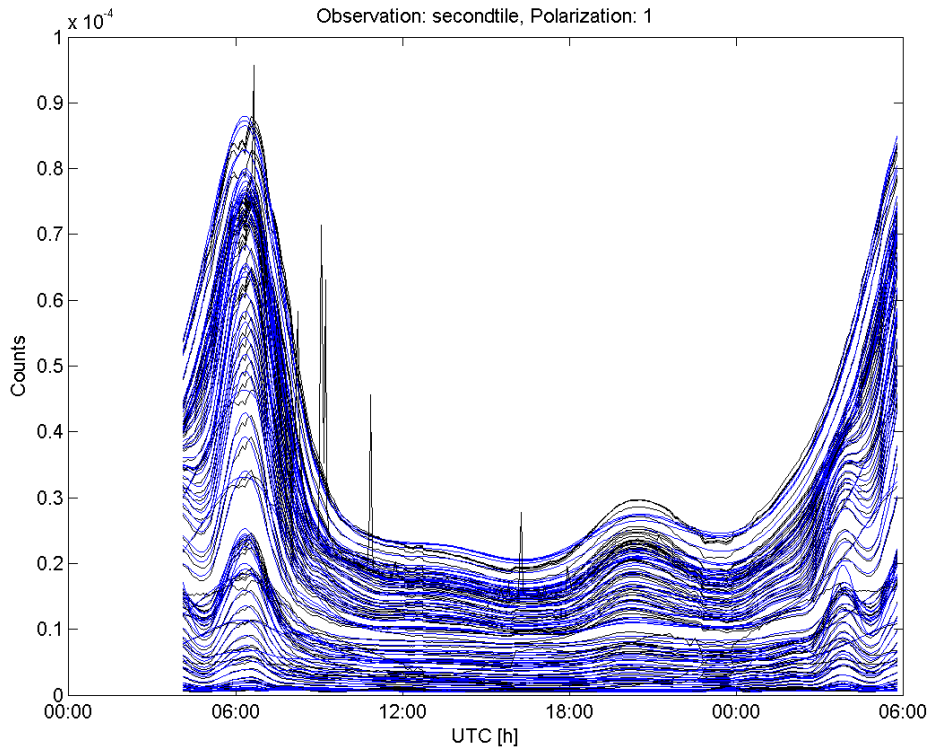
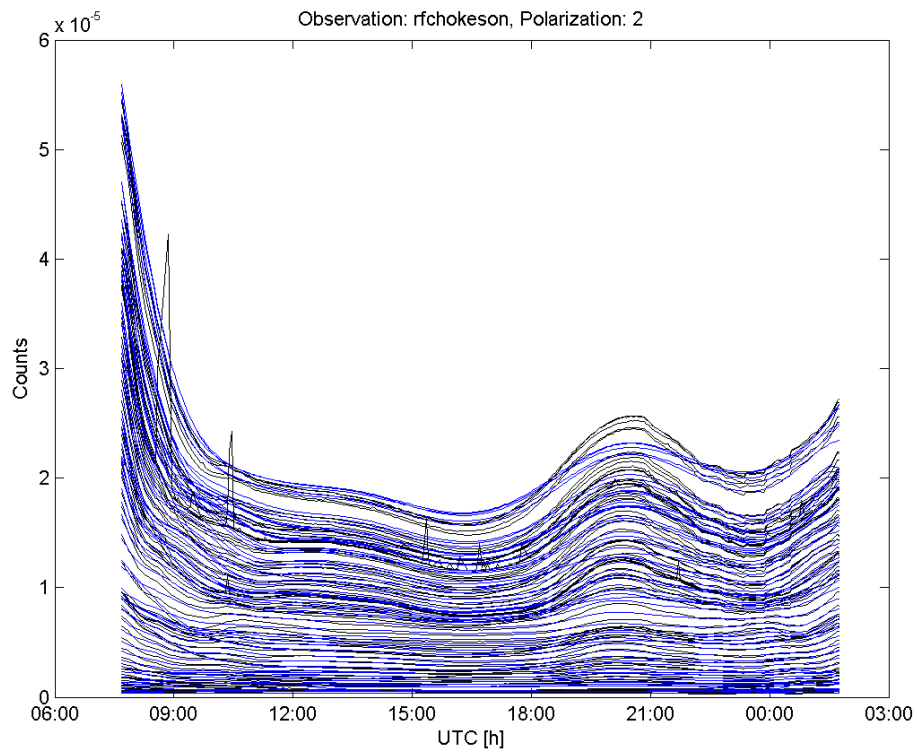
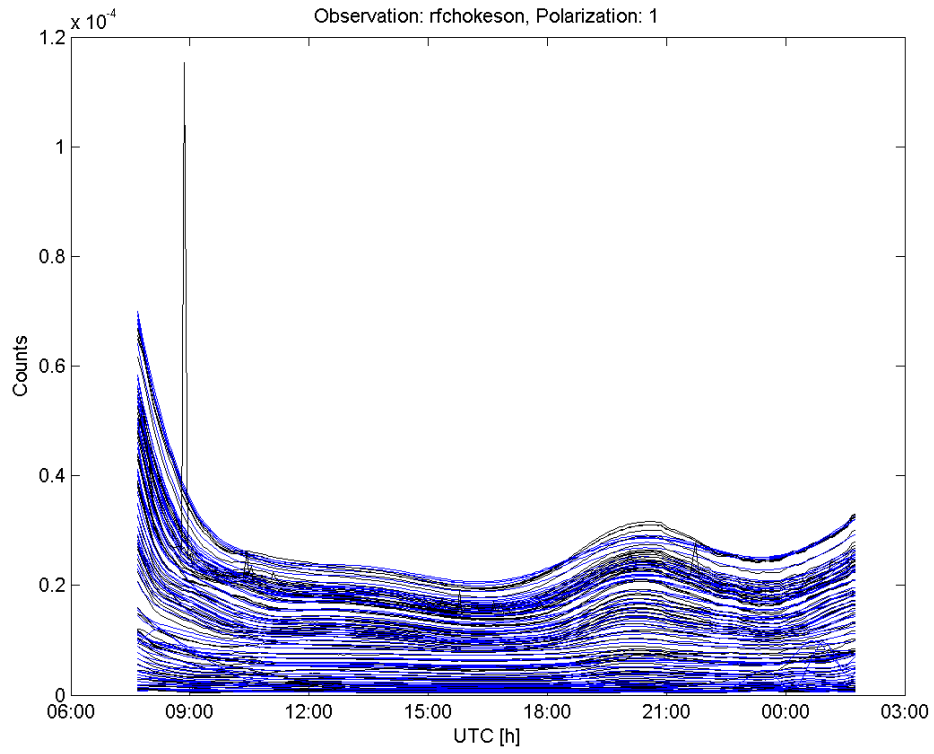


Figure 1. Typical 45-second integrated spectrum. Blue curve illustrates initial spectrum (with ADC overflow discarded). Black curve represents processed spectrum with median filter applied. Most of the narrow RFI spikes between 100 and 200 MHz are absent in the final processed spectrum, but the strong RFI around 250 MHz is still present.







2. Derived Model Parameters

In order to determine the gain and system temperature of the antenna tiles and beamformer from the drift scans, the following model was fit to the measurements:

$$N_{\text{driftscan}} = G * T_{\text{gal}} + S * T_{\text{sun}} + N_{\text{rcv}}$$

where:

1. $N_{\text{driftscan}}$ is the measured drift scan (as a function of UTC) in arbitrary power units (termed “counts”),
2. T_{gal} is the model of the expected contribution to the antenna temperature in K due to sky noise, and
3. T_{sun} is the model of the expected contribution to the antenna temperature in K due to a solar flux of 10^5 Jy (at all frequencies).

And fit parameters are given by

4. G , describing the gain of the system in units of counts/K, and includes the effects of both amplifier gains and the (frequency-dependent) reflection coefficient of the antenna impedance match to the first-stage amplifier in the LNA,
5. S , describing the strength of the sun in units of counts/K, and
6. N_{rcv} , describing the system noise (primarily due to the receiver) in counts.

From this model, the system temperature expressed as an equivalent sky brightness temperature is given by $T_{\text{sys}} = N_{\text{rcv}} / G$. The results of fitting this model to the *secondtile* drift scans are shown below and discussed in the next section. We treat S as a nuisance parameter. It is shown below for completeness, but does not play a significant role in the remainder of the analysis.

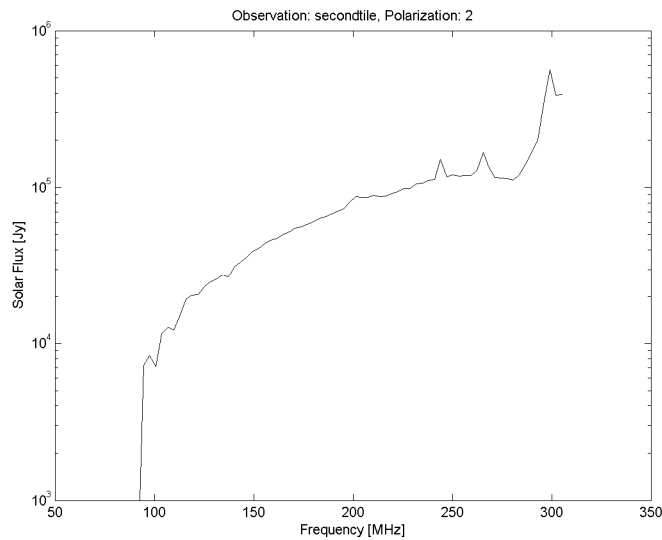
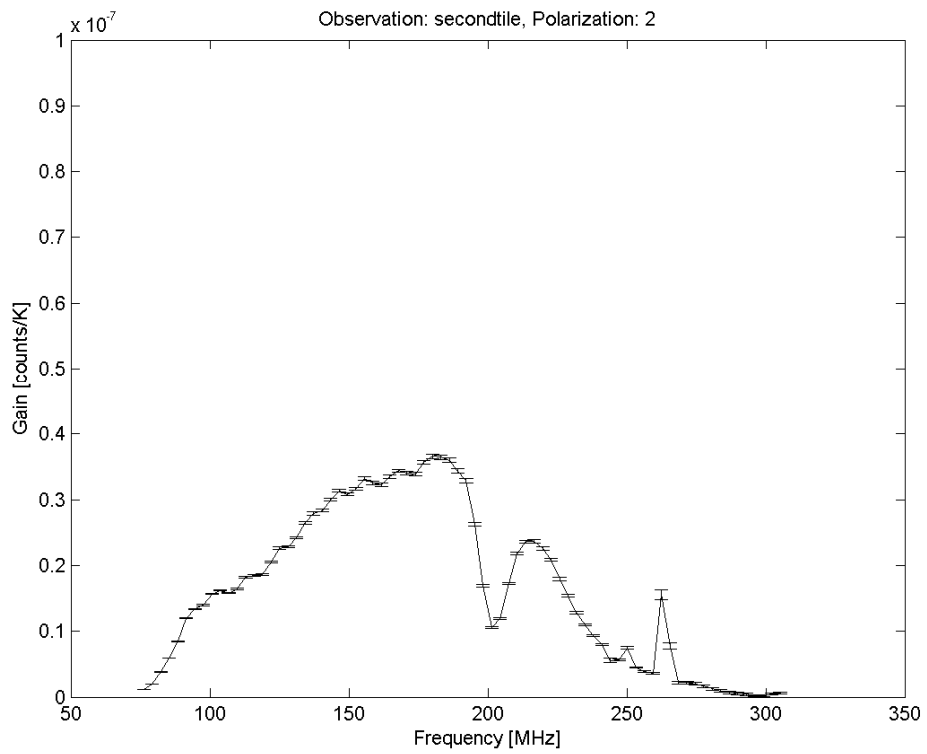
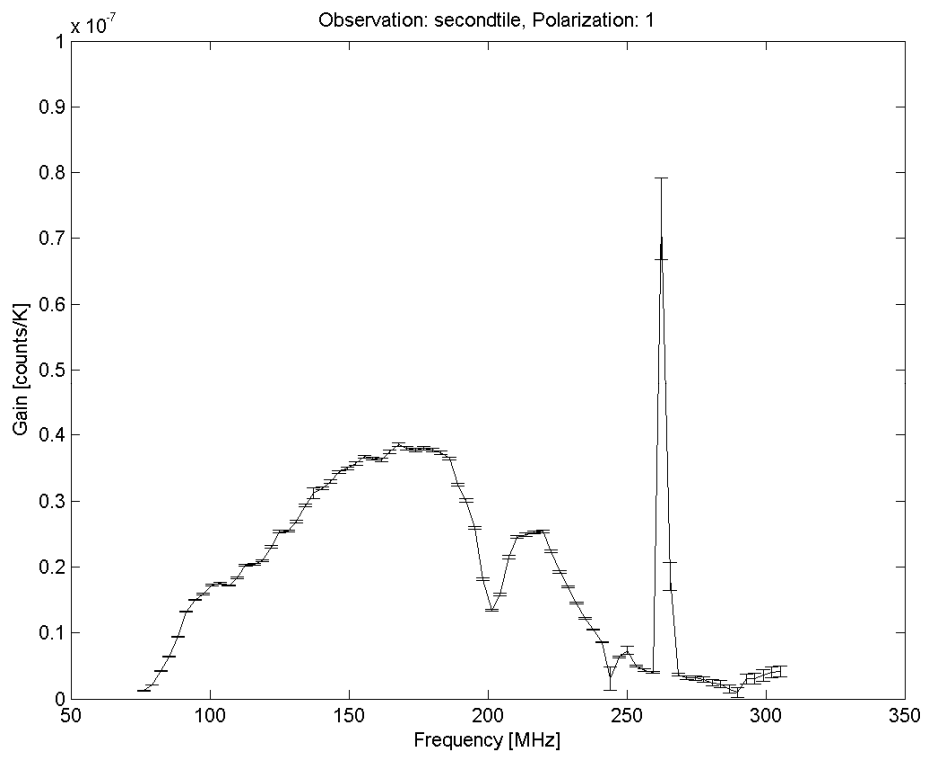
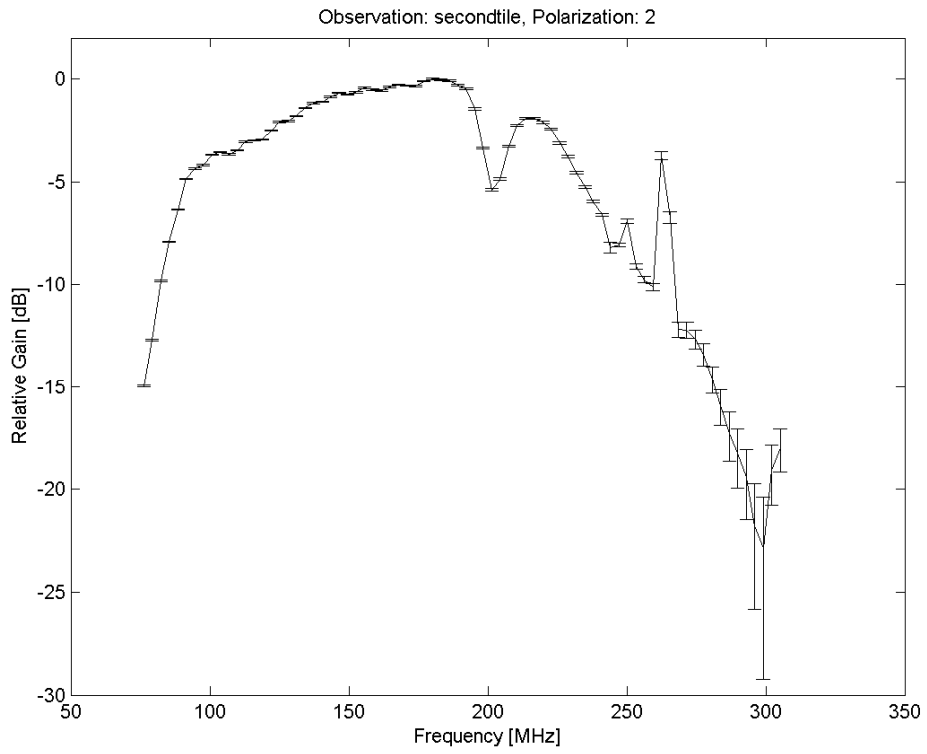
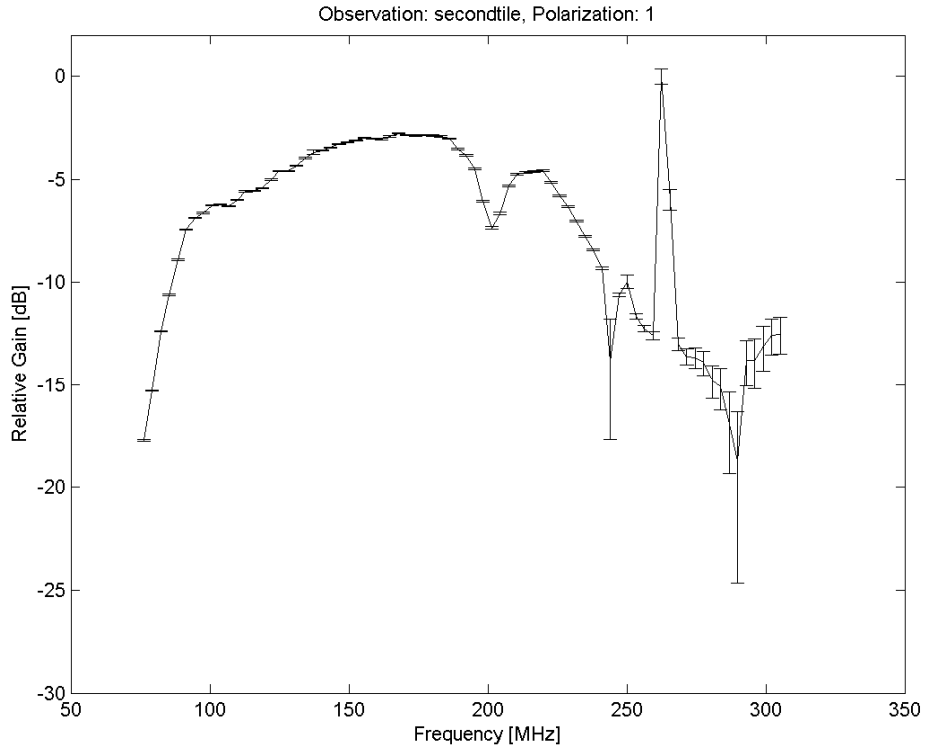
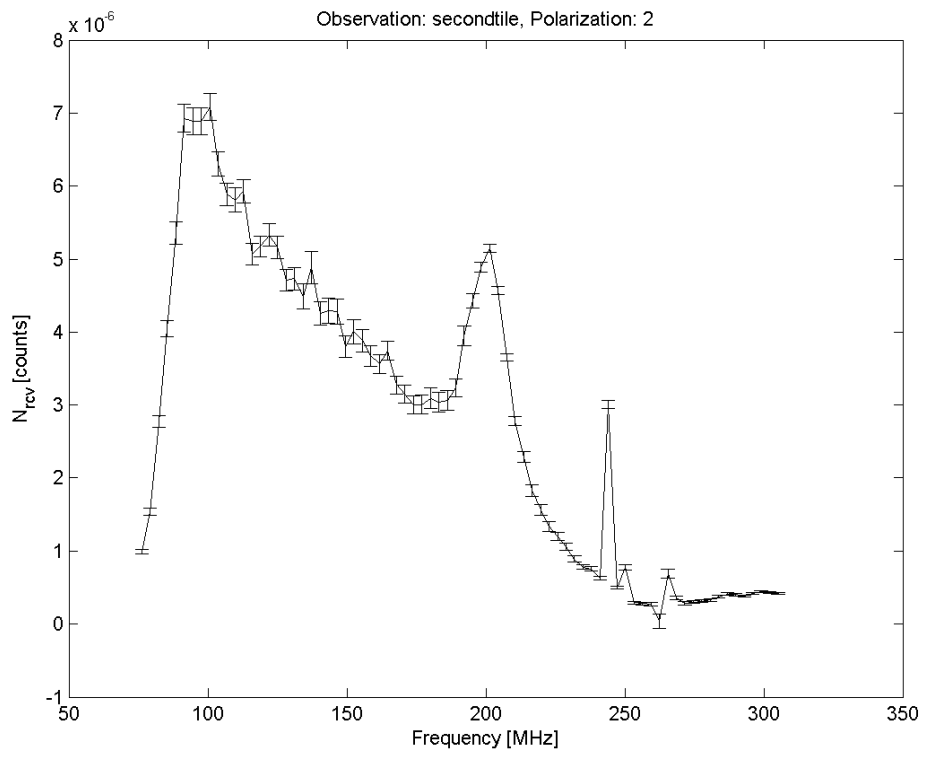
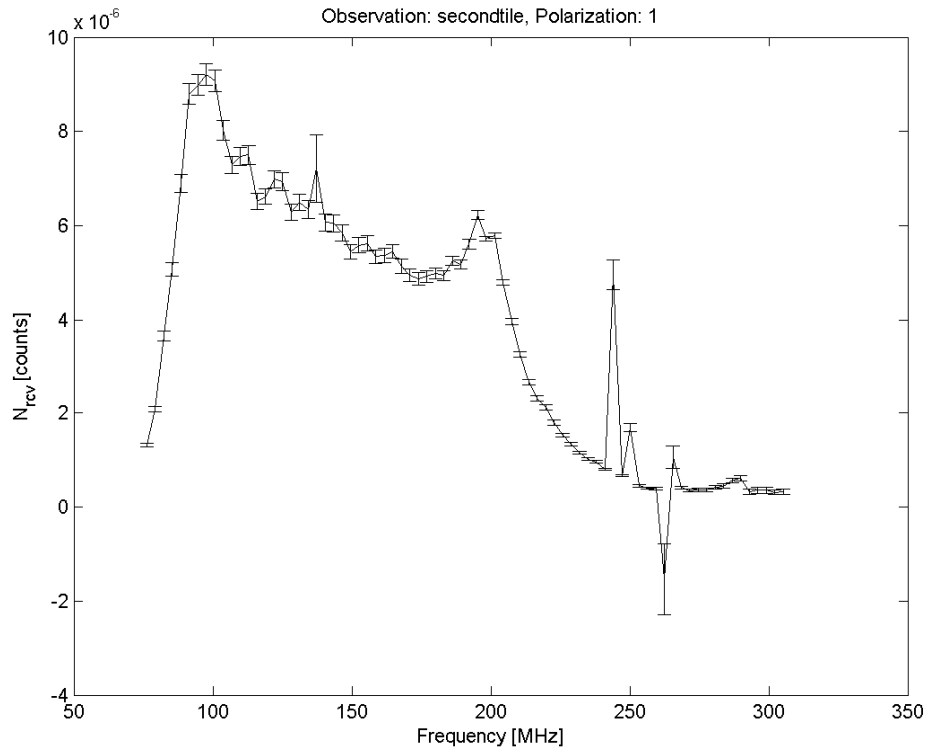
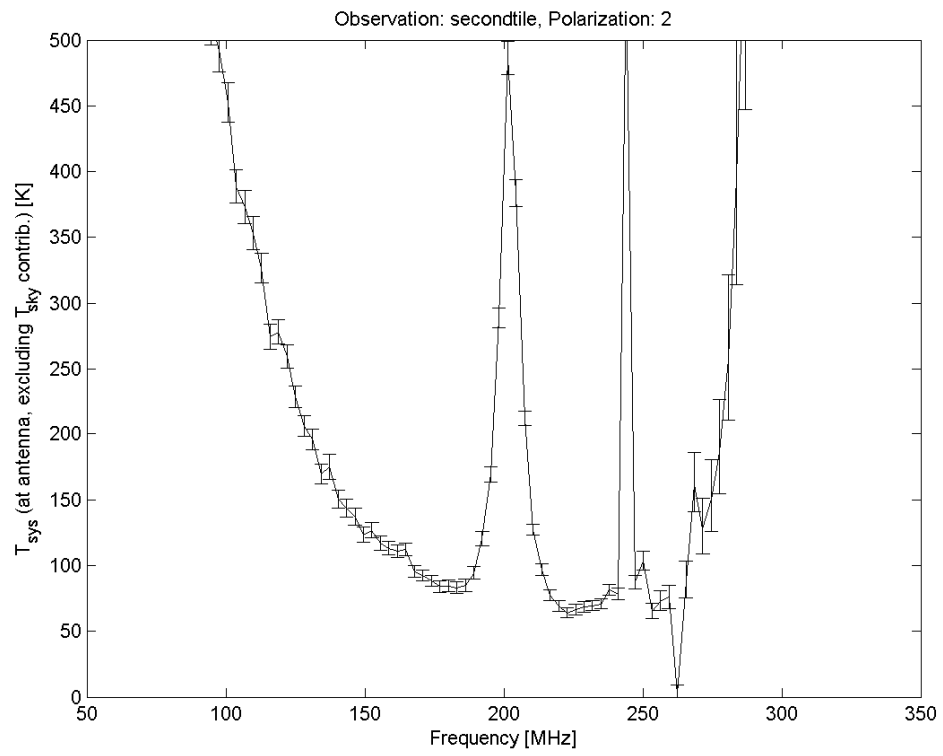
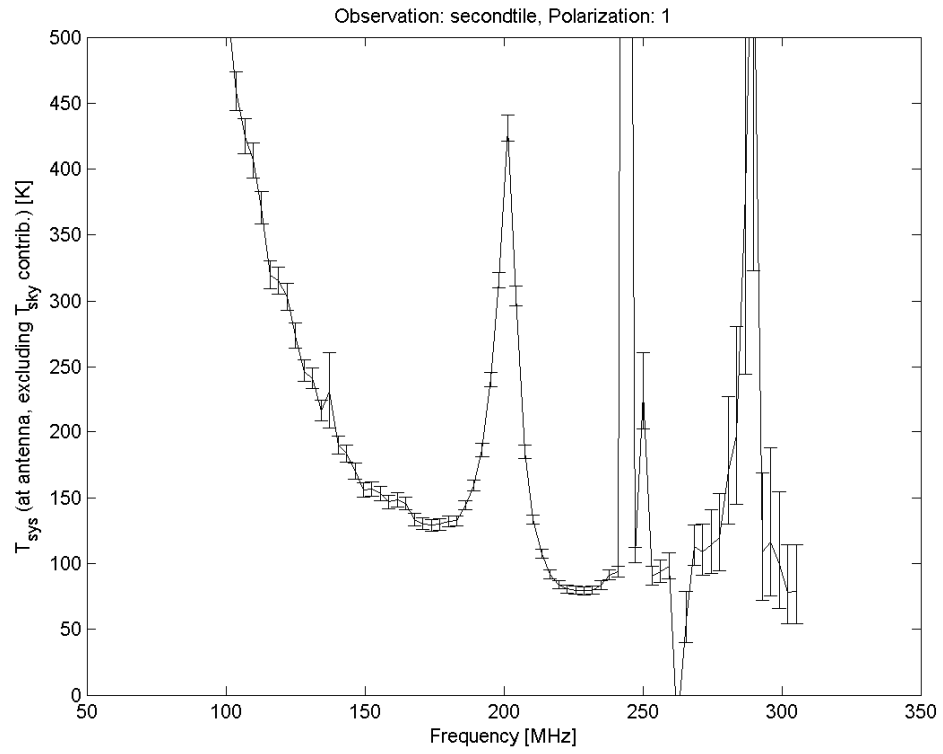


Figure 8. Solar flux in Jy derived from the model fit to the drift scans. The flux is in the range 104 to 105 Jy over the band, which is consistent with expectations. In general, I think the model fit slightly underestimates the strength of the sun due to the offset of the solar peaks in the modeled and measured drift scans.









3. Discussion of T_{sys}

The overall shape and level of the derived system temperature from the *secondtile* drift scans is within the generally expected bounds, particularly for polarization 2. The very large (~ 300 K) spike in system temperature at ~ 200 MHz is very troublesome as this corresponds to $z = 6$ in redshifted 21 cm observations. Hints of this feature have been seen in other measurements to characterize the antenna tiles. The earliest indication is from the Early Deployment drift scans. Bowman et al. 2007, their Figure 8, is reproduced as Figure 17 below and illustrates a similar peak in T_{receiver} (same as our T_{sys}) in the top panel. (Note that “gain” plotted in that figure is the inverse of our gain, G .) These measurements, however, were not definitive due to the use of a damaged beamformer unit in the field. The apparent frequency of the peak is somewhat higher in these results.

More recent tests of an antenna tile in an anechoic chamber at Lincoln Laboratories produced a \sim few dB drop in gain at 205 MHz, as shown in Figure 18 below. A similar drop in gain is also visible as the notch at 203 MHz in the example drift scan spectrum in our Figure 1. The frequency of the feature seen at Lincoln Labs appears to be slightly higher than the present results, but the spectrum was only sampled in 5 MHz intervals in the anechoic chamber, so it is difficult to make a real comparison. One speculation that fits the apparent change in frequency comes from the fact that the shift is in accordance with what would be expected due to the change in dipole spacing from 1.07 to 1.10 m, if the feature were due to mutual coupling between neighboring dipole elements.

A characterization of the notch amplitudes in the processed drift scan spectra is provided in Figures 19 and 20. From these plots, it is evident that the amplitude of the notch is essentially proportional to the received power at 203 MHz, with an offset such that the notch has zero amplitude at approximately (and presumably coincidentally) the minimum power level recorded during the drift scans (at times when the coldest parts of the sky were passing through the antenna beam). From these measurements, we would expect the notch to be seen as a bump (excess power) if the coldest sky temperatures were only slightly lower than observed. Unfortunately, I do not believe there is an easy way to produce such a measurement (since we have no control of the sky temperature!) and using some kind of absorber would still produce an antenna temperature of order ~ 300 K.

New antenna modeling providing complete electromagnetic simulations of the full antenna tiles motivated by the confirmation of this feature is underway by Alan Rogers and Randall Wayth. They have already reproduced the feature and have begun to provide a compelling explanation for its presence. Preliminary results suggest that vertical currents in the outer struts of the dipole batwings are responsible for creating a mutual coupling between multiple elements. Discussion of these results will be the subject of other memoranda (see already EDGES memorandum #37 by Alan Rogers).

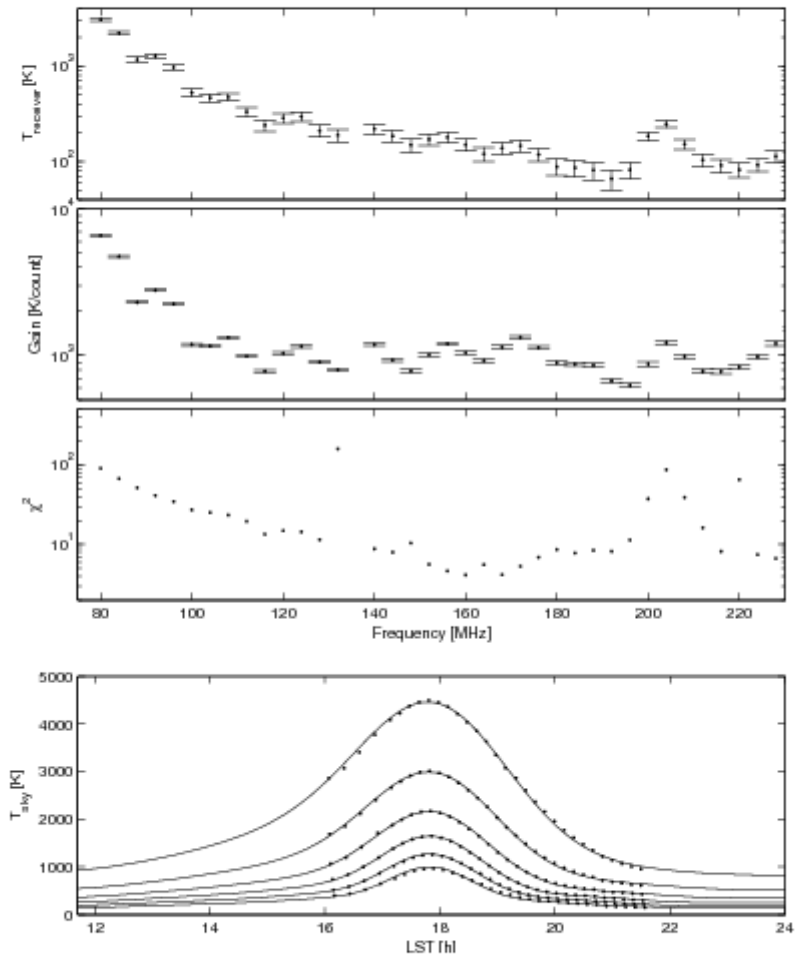


Figure 17. Results of drift scans with the Early Deployment system show a similar peak in the system temperature at about 200 MHz. Reproduced from Bowman et al. 2007, their Figure 8.

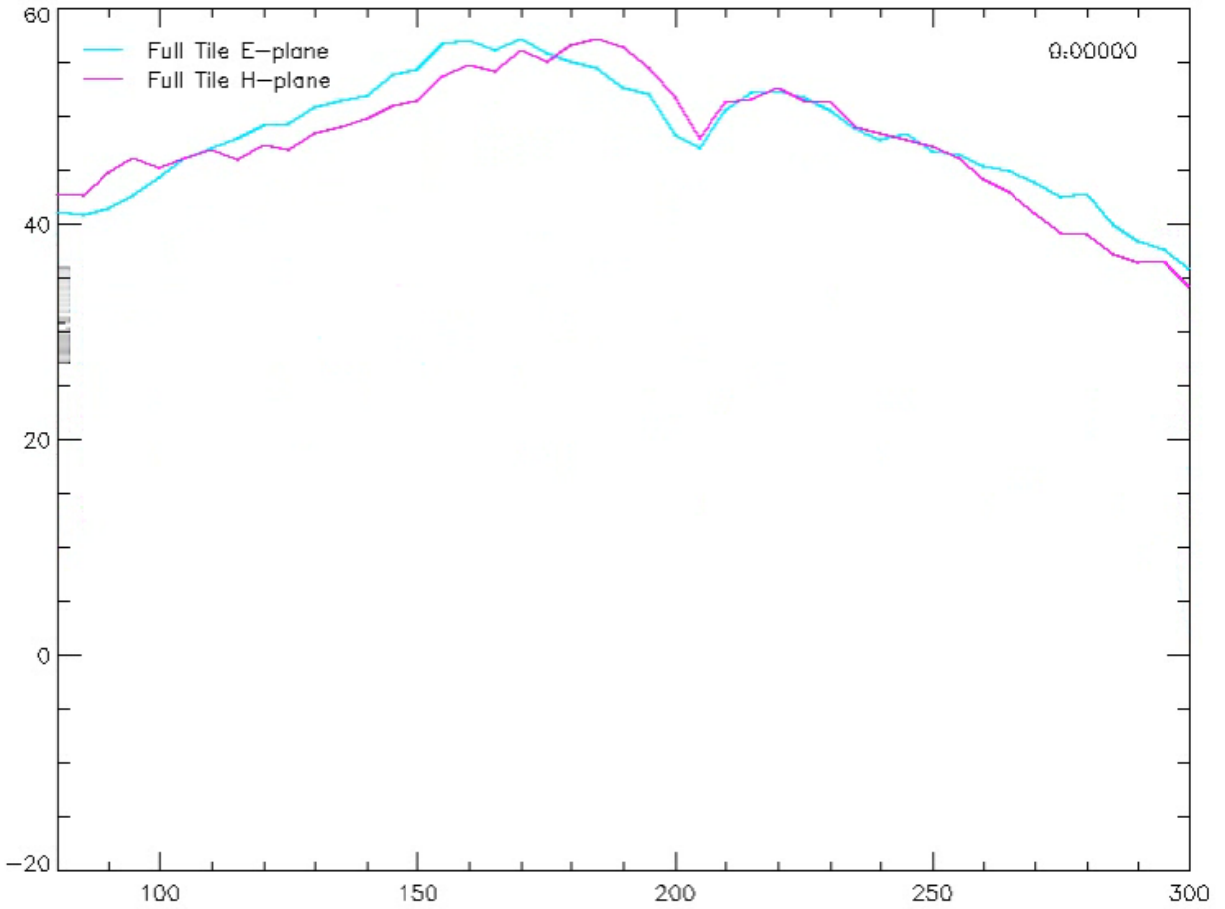


Figure 18. Antenna tile bandpass at zenith derived from anechoic chamber tests at Lincoln Laboratory. Note the notch in the gain at ~200 MHz. Plot provided by Chris Williams.

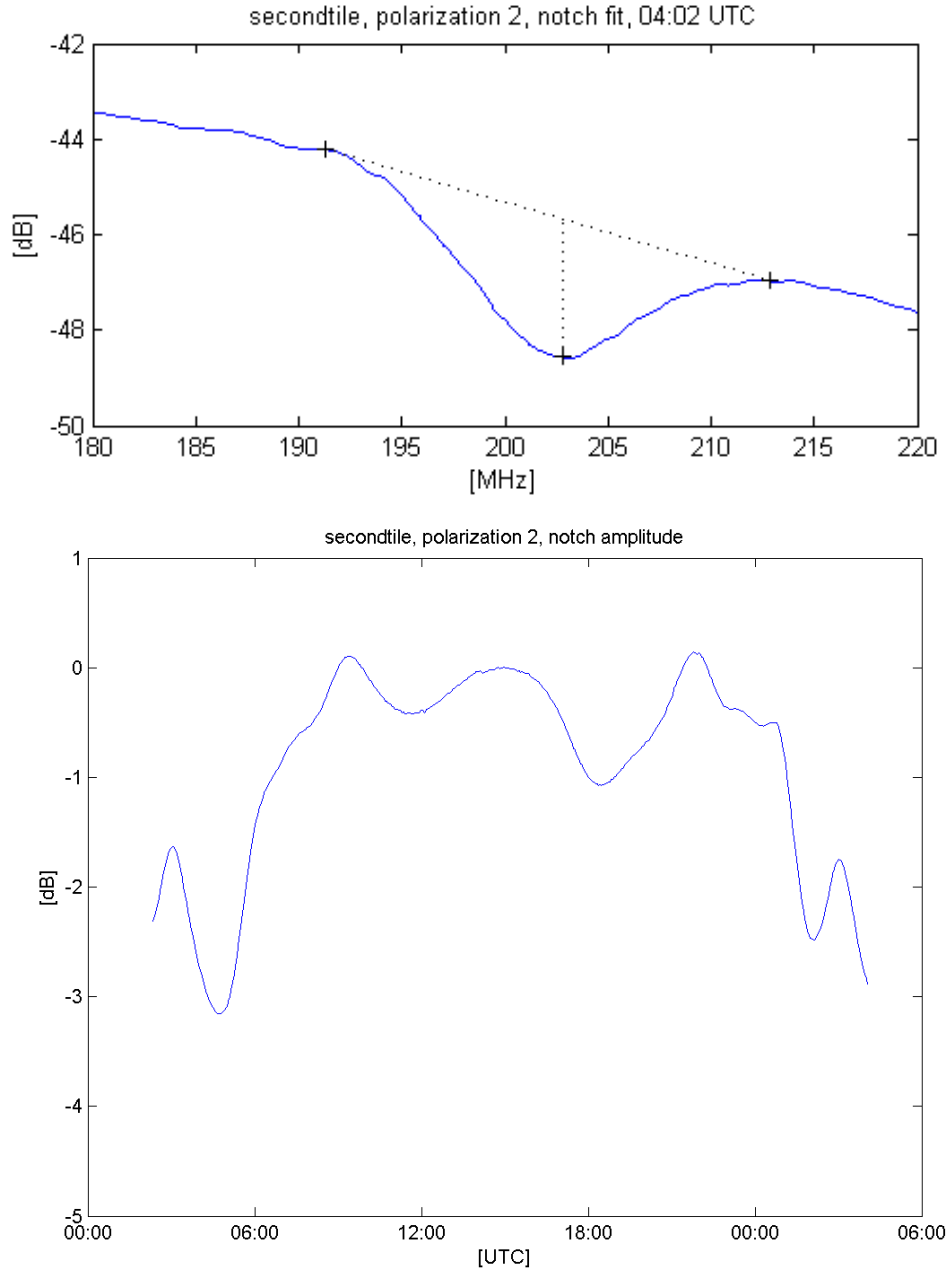


Figure 19. The *top panel* shows an illustration of the notch amplitude calculation at 04:02 UTC (the end of the observations), when the notch was very pronounced. A linear interpolation was performed between the channel power values at 191 and 213 MHz, and the difference was calculated between the “expected” (interpolated) power and the actual measured channel power at the approximate center of the notch at 203 MHz. The *bottom panel* plots the difference as a function of UTC. The difference is greatest (up to approximately -3 dB) when the Galactic center is overhead and nearly disappears when the cold sky is overhead.

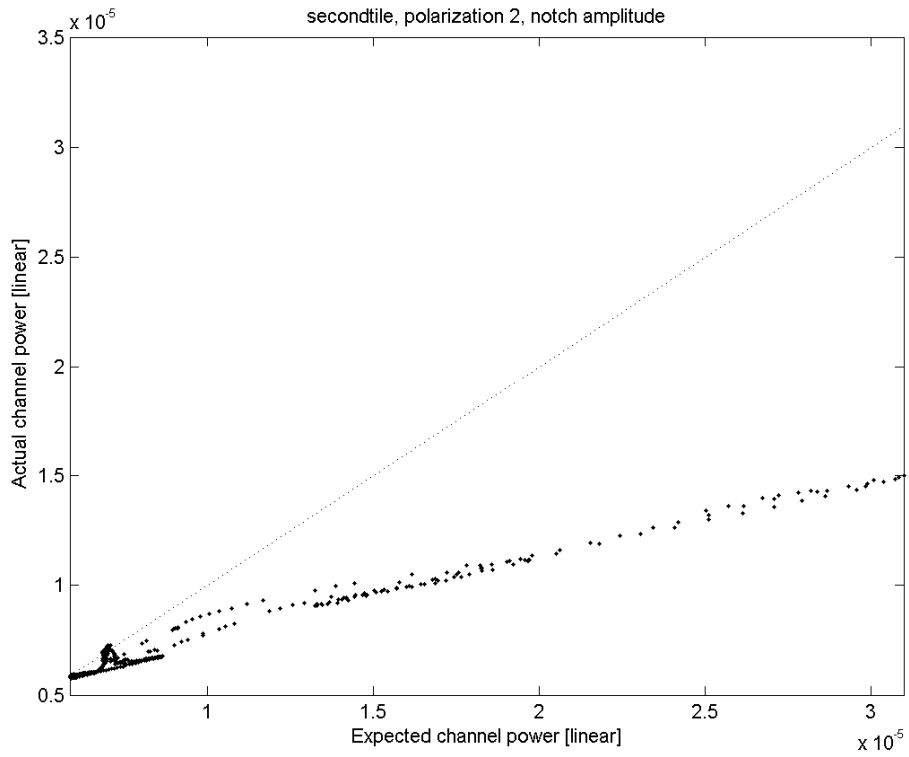


Figure 20. Comparison between the expected (interpolated) channel power and the actual measured channel power at 203 MHz. The dotted line is a guide showing the line for equality. There is a clear linear relation, demonstrating that the amplitude of the notch is proportional to the receiver power and intersects the expected power at approximately the minimum power level recorded during the drift scan.

3.1. T_sys and T_sky

Including a typical value for a cold region of the Galactic emission given by:

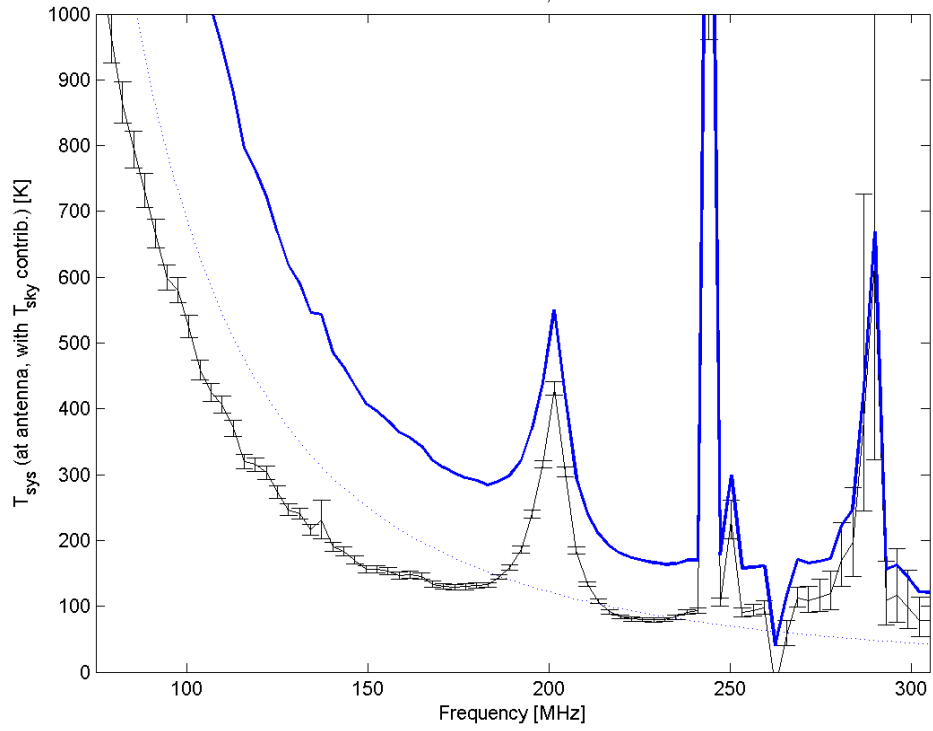
$$T_{\text{sky}} = 250 \cdot (f / 150 \text{ MHz})^{-2.5} \text{ K}$$

in with the derived (receiver noise only) T_sys gives an estimate of the total system temperature for an EOR observation. This is shown in Figures 21 and 22 and listed in Table 1.

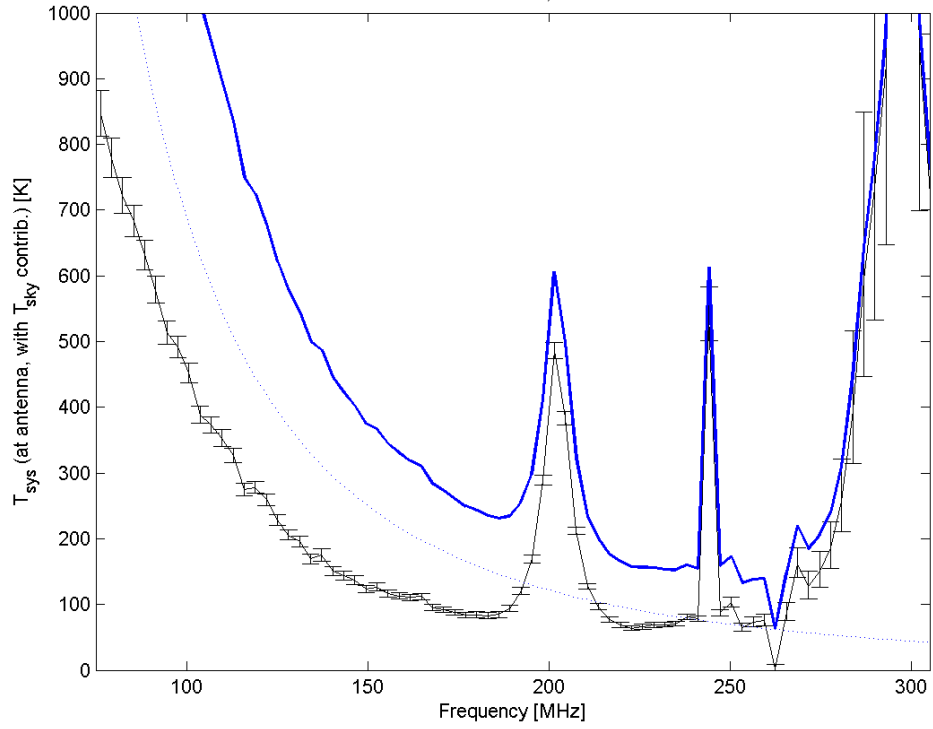
Table 1. T_sys (*secondtile*, polarization 2) and T_sky as Functions of Frequency

Freq [MHz]	T_sys [K]	T_sky (cold) [K]	T_sys + T_sky [K]				
76.3	846.9	1356.2	2203.1	161.7	110.7	207.1	317.8
79.3	779.0	1229.5	2008.4	164.8	112.0	197.7	309.7
82.4	722.2	1118.7	1840.9	167.8	95.2	188.8	284.0
85.4	682.9	1021.5	1704.3	170.9	92.4	180.5	272.9
88.5	631.7	935.6	1567.3	173.9	88.4	172.7	261.1
91.5	578.4	859.6	1438.0	177.0	84.0	165.3	249.3
94.6	513.7	791.9	1305.6	180.0	84.4	158.4	242.8
97.6	492.3	731.5	1223.7	183.1	83.2	151.9	235.1
100.7	452.6	677.3	1129.9	186.1	85.0	145.7	230.7
103.7	388.8	628.6	1017.3	189.2	94.1	139.9	234.1
106.8	373.0	584.6	957.6	192.2	120.2	134.4	254.7
109.8	353.3	544.8	898.2	195.3	169.2	129.3	298.5
112.9	326.4	508.8	835.2	198.3	288.9	124.3	413.3
115.9	274.3	475.9	750.2	201.4	486.5	119.7	606.2
119.0	278.0	446.0	724.0	204.4	383.4	115.3	498.6
122.0	259.5	418.6	678.1	207.5	211.8	111.1	322.8
125.1	228.0	393.6	621.6	210.6	127.3	107.1	234.4
128.2	205.9	370.6	576.5	213.6	96.8	103.3	200.1
131.2	195.8	349.4	545.2	216.7	77.2	99.7	176.9
134.3	169.5	329.9	499.4	219.7	69.2	96.3	165.5
137.3	175.0	311.8	486.9	222.8	64.0	93.0	157.0
140.4	150.4	295.2	445.5	225.8	66.5	89.9	156.4
143.4	143.4	279.7	423.1	228.9	68.6	86.9	155.5
146.5	136.9	265.4	402.2	231.9	69.3	84.1	153.4
149.5	123.4	252.0	375.4	235.0	70.9	81.4	152.3
152.6	126.8	239.6	366.4	238.0	81.3	78.8	160.1
155.6	117.0	228.0	345.1	241.1	78.4	76.3	154.8
158.7	113.2	217.2	330.4				

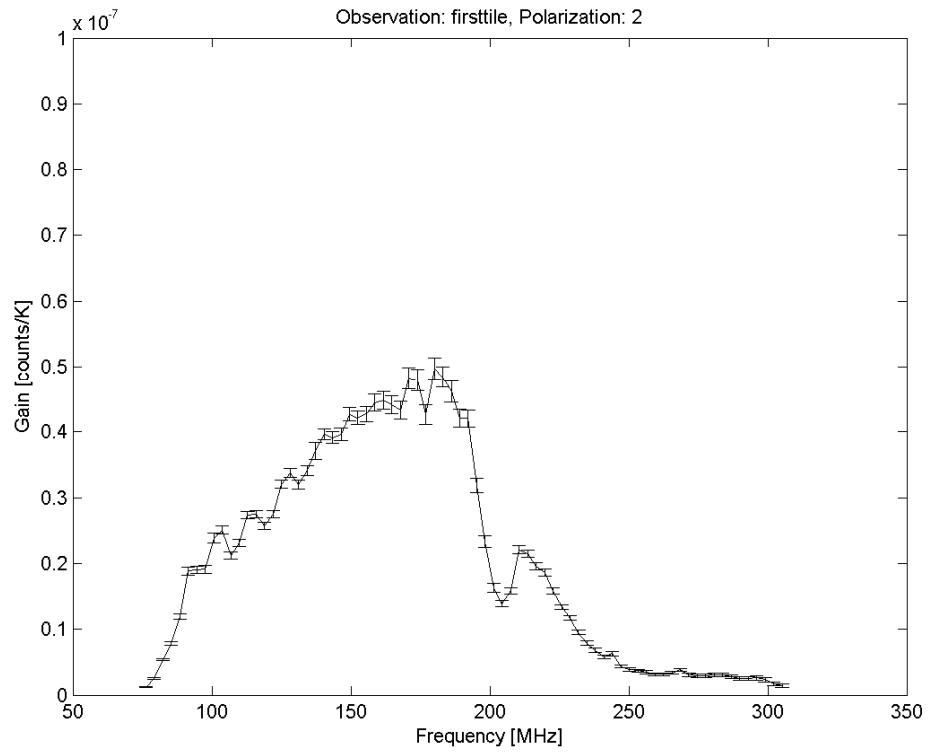
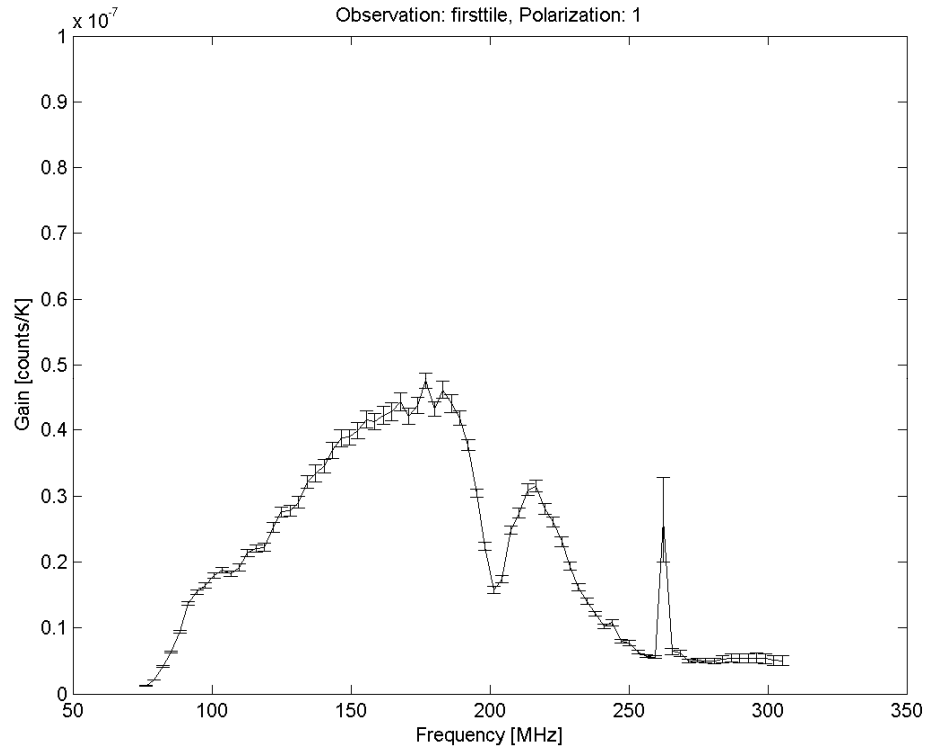
Observation: secondtile, Polarization: 1



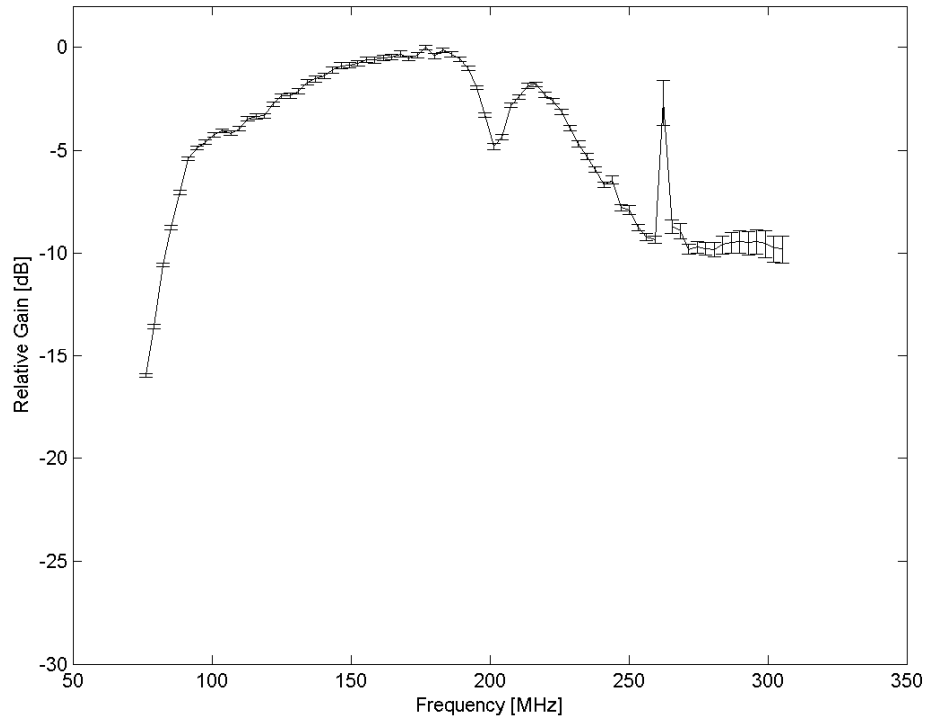
Observation: secondtile, Polarization: 2



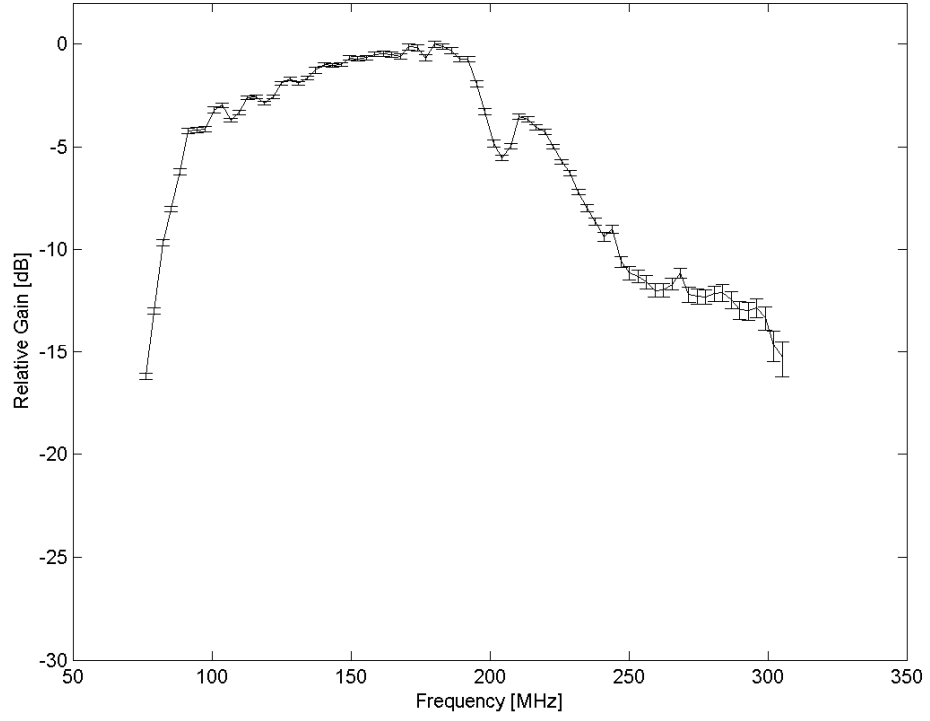
4. Fits from *firsttile* and *rfchokeson*

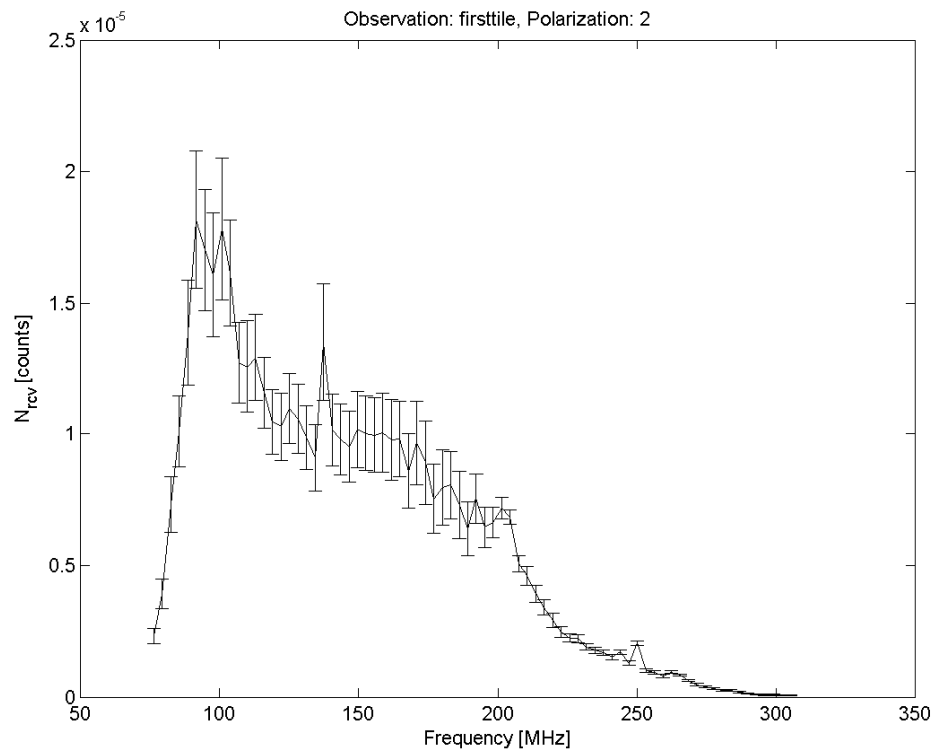
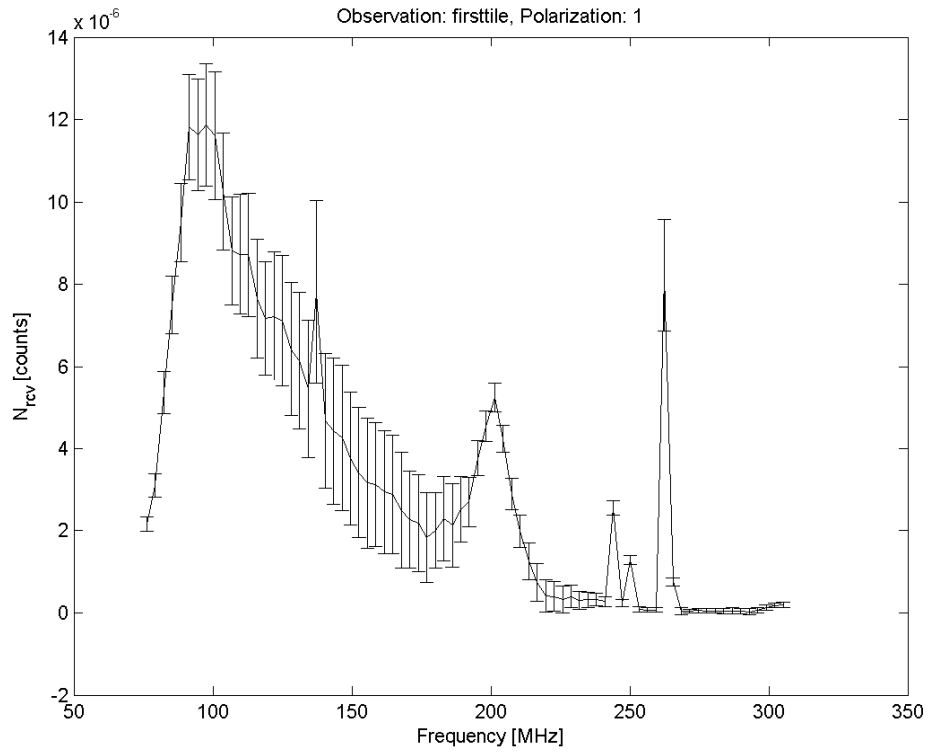


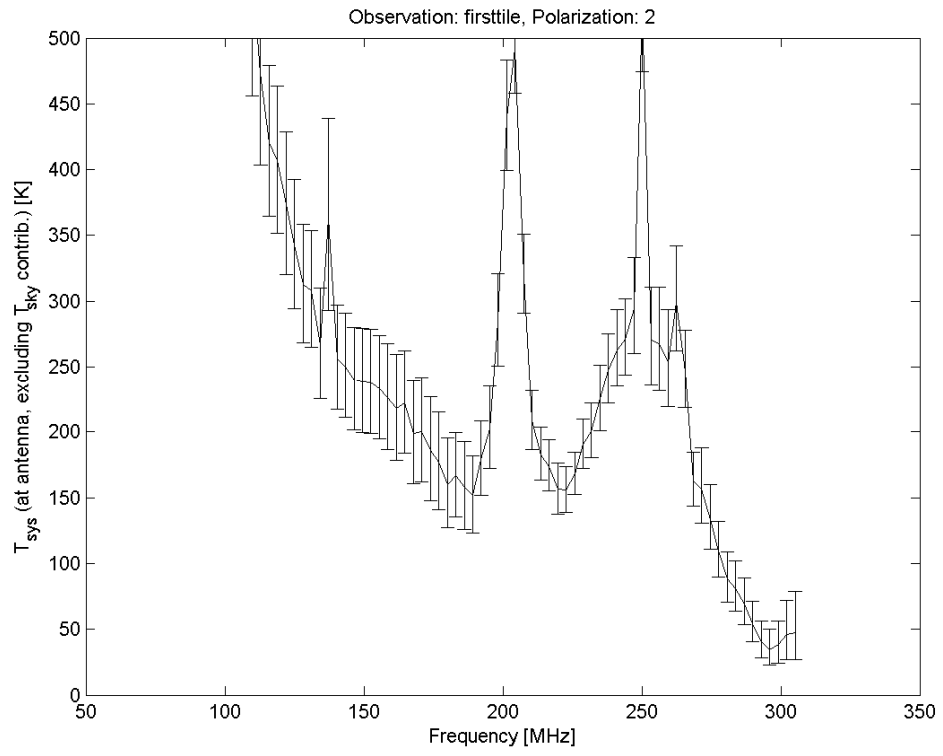
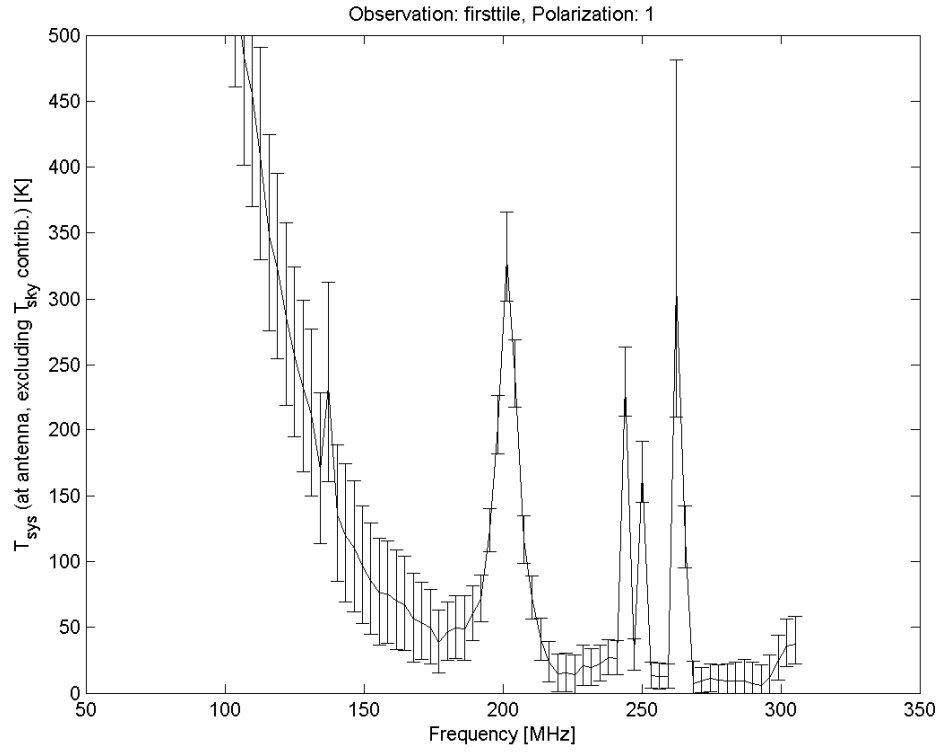
Observation: firsttile, Polarization: 1

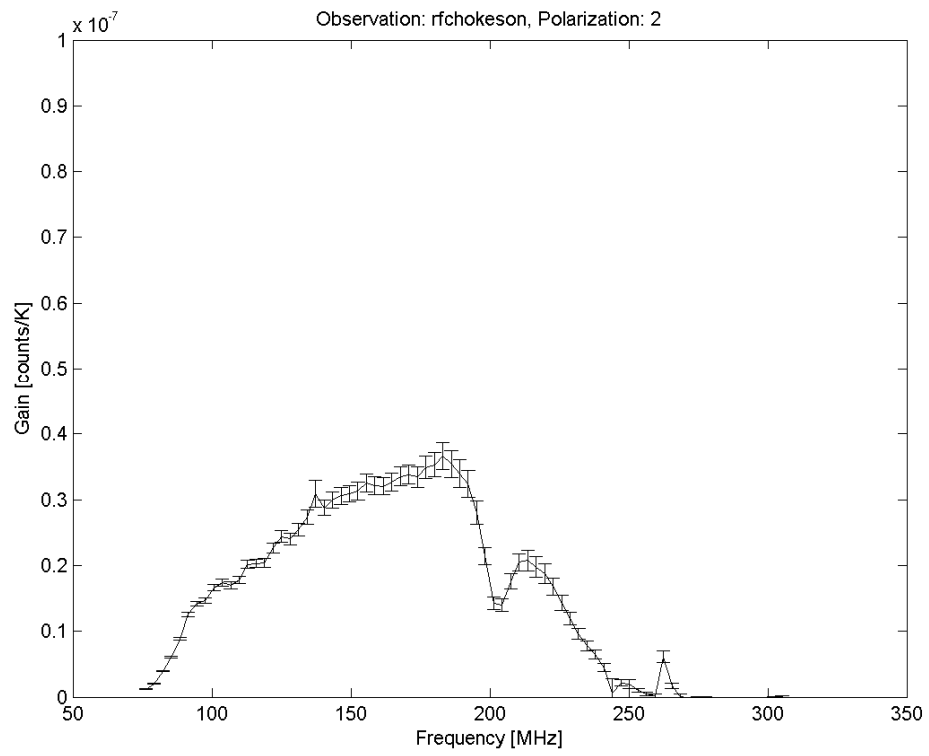
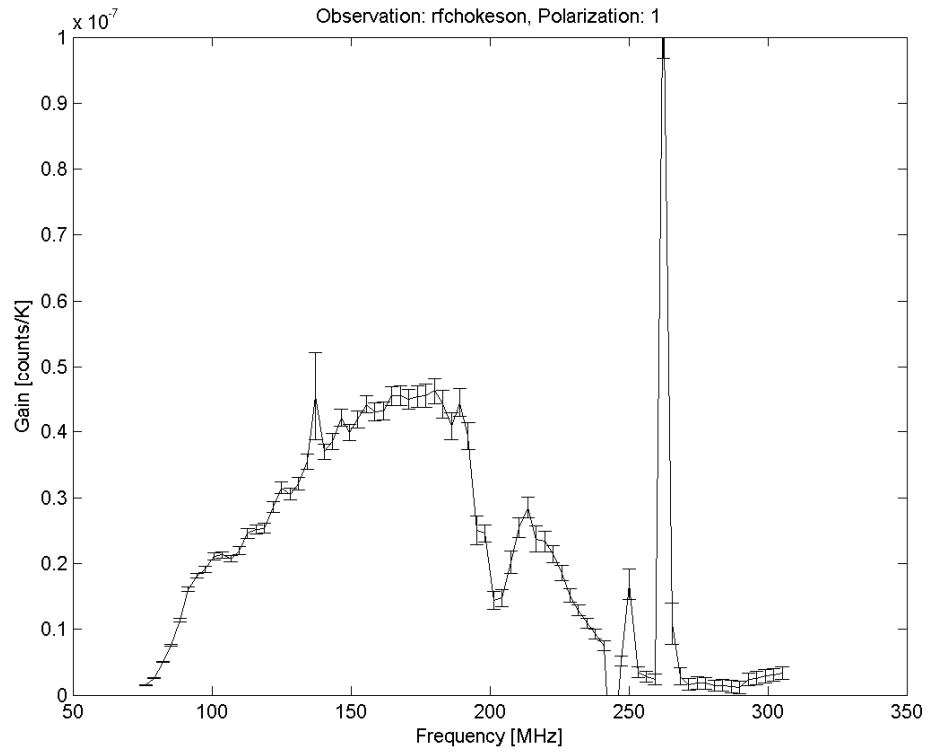


Observation: firsttile, Polarization: 2

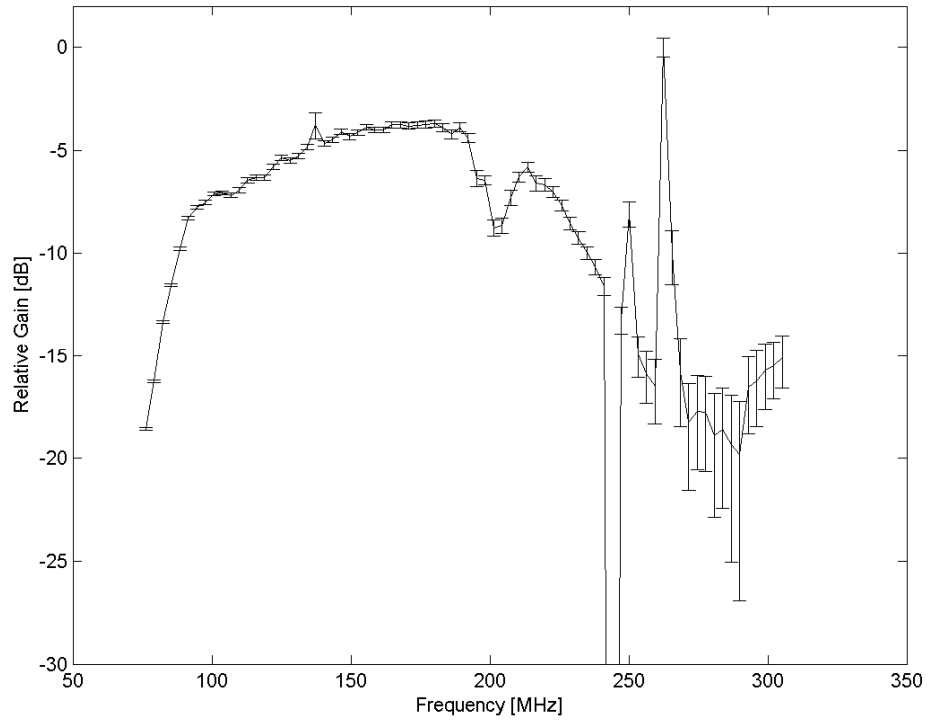




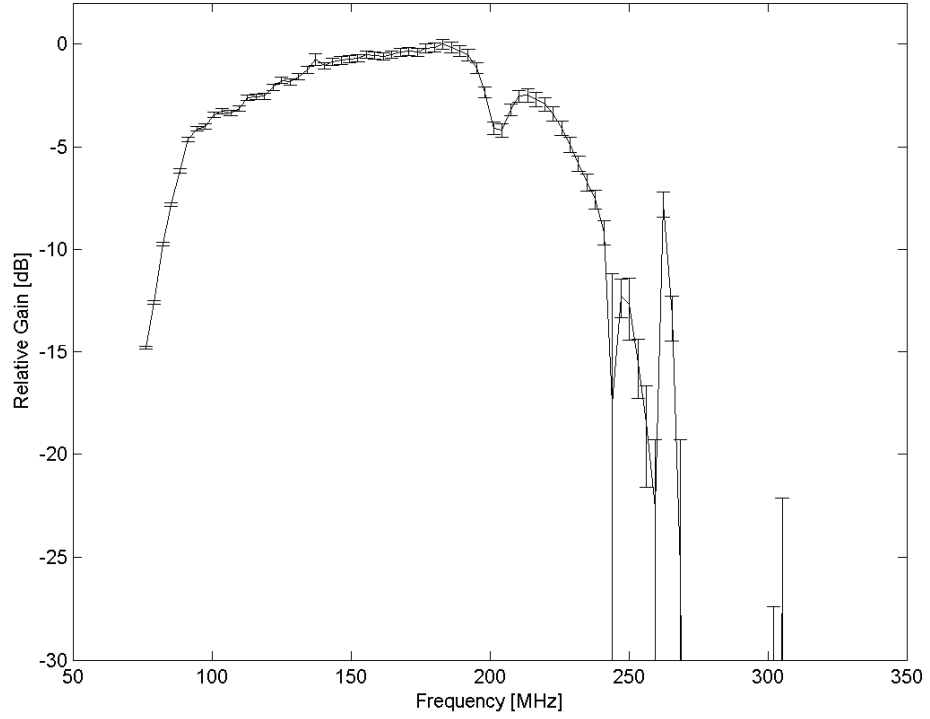


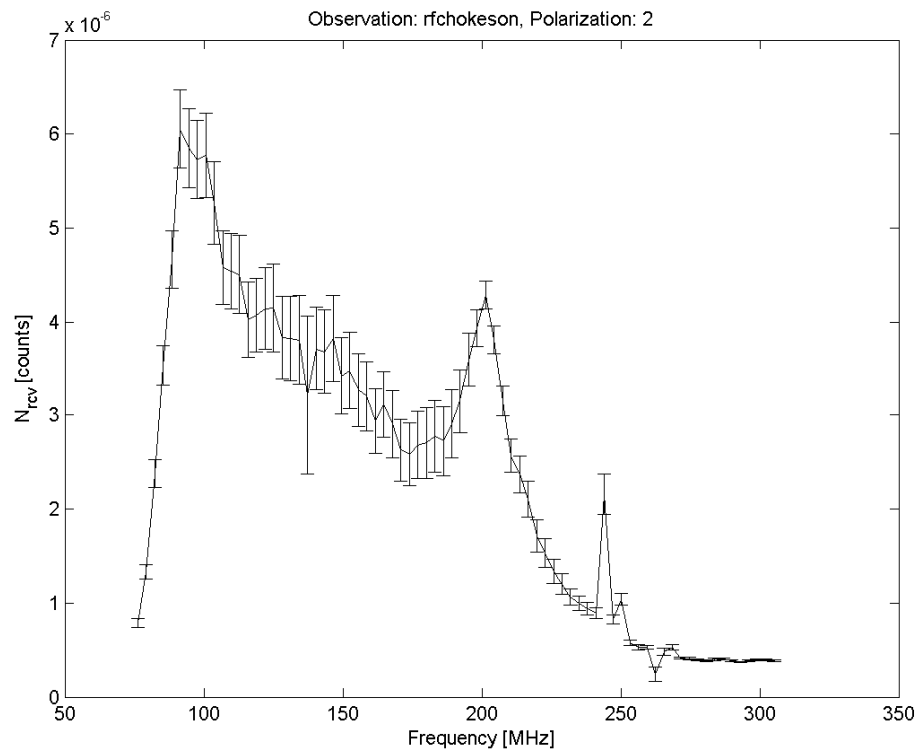
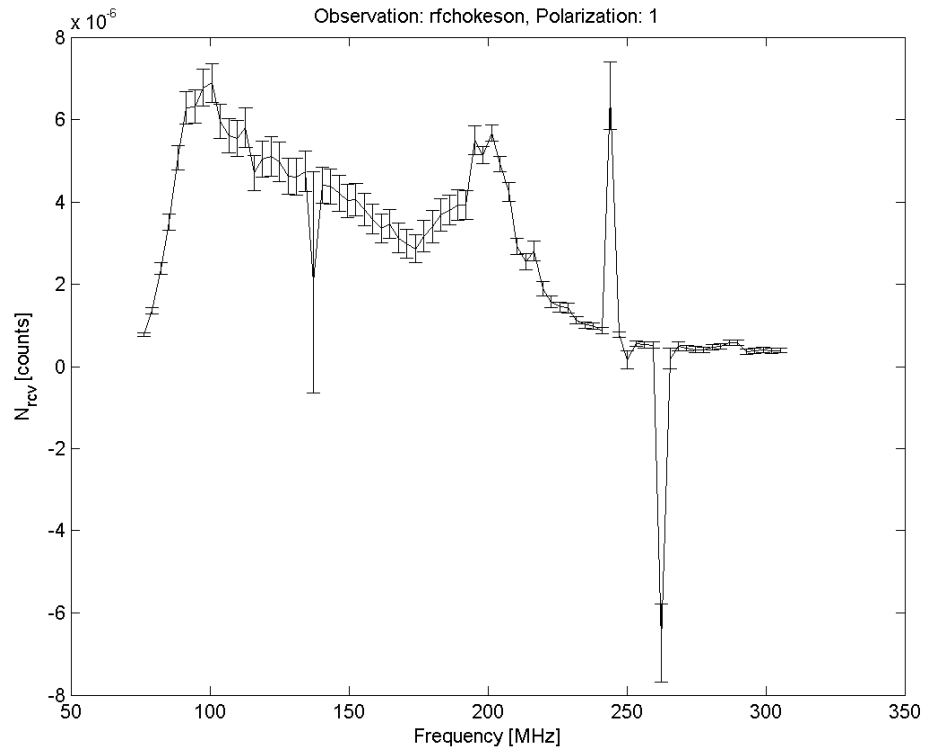


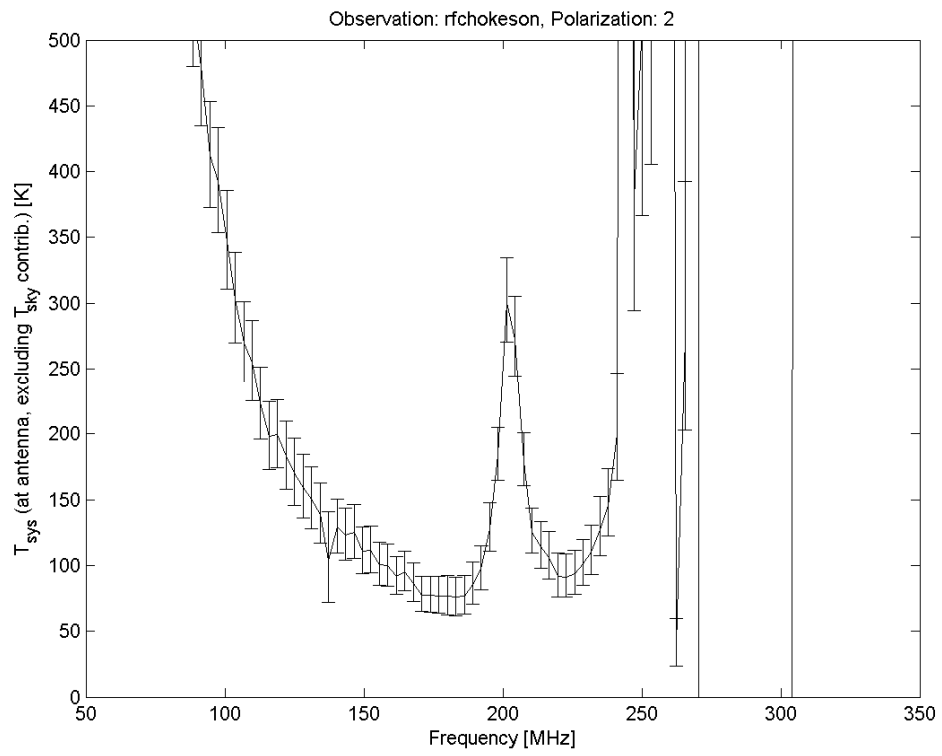
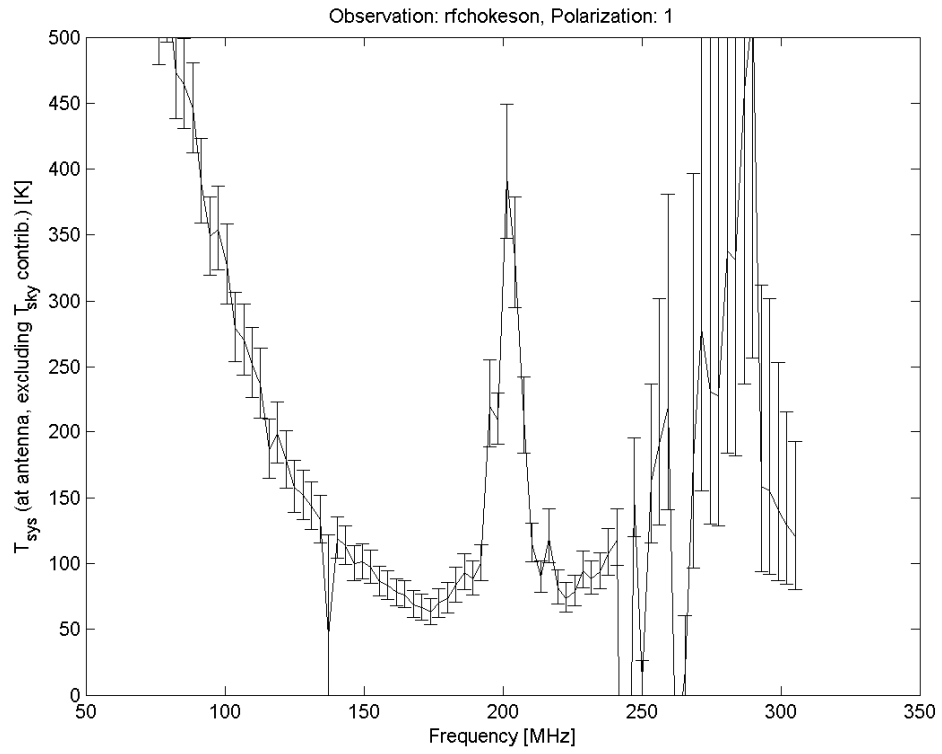
Observation: rfchokeson, Polarization: 1



Observation: rfchokeson, Polarization: 2







5. Acknowledgements

This analysis was supported in many ways by the contributions of Frank Briggs, Brian Corey, Chris Williams, and the X1 field deployment team.

6. References

1. EDGES memoranda #30-33, 37:
http://www.haystack.mit.edu/ast/arrays/Edges/EDGES_memos/EdgesMemo.html
2. C. G. T. Haslam, H. Stoffel, C. J. Salter, and W. E. Wilson. A 408 MHz all-sky continuum survey. II - The atlas of contour maps. *A&AS*, 47:1 — +, January 1982.